A High Performance Pneumatically Actuated Soft Gripper Based on Layer Jamming

Xianpai Zeng

Design Inovation and Simulation Laboratory, Department of Mechanical Engineering, Ohio State University, Columbus, OH 43210

e-mail: zeng.108@osu.edu

Hai-Jun Su¹

Professor Fellow ASME

Design Inovation and Simulation Laboratory, Department of Mechanical Engineering,

Ohio State University, Columbus, OH 43210 e-mail: su.298@osu.edu

This article presents a novel soft robotic gripper with a high payload capacity based on the layer jamming technology. Soft robots have a high adaptability, however suffer a low payload capacity. To overcome these conflicting challenges, here we introduce a 3D printed multi-material gripper that integrates jamming layers for enhancing payload capacity. By inflating the internal air chamber with positive pressure, the finger can be actuated to a large bending angle for adapting complex shapes. Layers of jamming sheets are bounded on the finger structure and are then sealed inside a vacuum bag. When a high payload is desired, air inside the vacuum bag is drawn out and a negative air pressure is applied to the jamming layers, which leads to the gripper locked at the actuated shape. To evaluate the performance of the gripper, we conducted extensive tests including actuation, stiffness variation, typical payload capacity, and adaptability. The results show that our gripper is not only highly adaptable just like most soft grippers but also more importantly capable of grasping heavy (about 6-10 kg) objects comparable to rigid-body counterparts. [DOI: 10.1115/1.4053857]

Keywords: compliant mechanisms, grasping and fixturing, robot design, soft robots

1 Introduction

Soft robots have been a widely studied solution to numerous complex tasks that require high adaptability [1,2]. For the soft robots to interact with environments in a safe manner, materials such as textiles, elastomers, or any other highly flexible materials are used [3]. Due to the materials' flexibility, soft robots are less likely to damage fragile payloads or cause human injuries [1,4]. Soft robots also have the advantages including low cost, light weight, and easy customization for different applications [5]. However, there are some limitations associated with their high compliance. Actuators based on smart materials are limited on driving strokes and loading capacities [6]. Tendon-driven grippers require

sophisticated control algorithm [7]. Additionally, soft actuators tend to have undesired large deformation under external loads.

To enhance load carrying capability of soft actuators, interest has been drawn to exploring variable stiffness technologies. Blanc et al. [8] classify controllable stiffness methods based on the change in intrinsic properties, either the geometry-related or material-related ones. However, the solutions from the two categories have issues including high system complexity [9], low durability [10], and low strength [11].

Increasing attention has been drawn to locking-based solutions. Jamming solutions control the interactions of locking mediums contained in the seal volume. Friction force among the locking mediums is related to applied force or pressure. The structure's stiffness can be controlled as the result of the tunable interaction. Extensive studies have been done on granular jamming [12-17] and fiber jamming [18]. However, these designs have relatively low stiffness change. In contrast, layer jamming [19–26] has shown potential for achieving high stiffness change. Kim et al. [20,21] developed a surgery manipulator using layer jamming which can assume a flexible state for insertion without causing injury and a stiff state for high positional accuracy. Zeng et al. [27] designed a parallel-guided mechanism with layer jamming and proposed a mathematical model to describe the stiffness change. Gao et al. [28] proposed a cabledriven gripper with three fingers equipped with layer jamming which achieves good load capacity enhancement. However, using both servo motors and pneumatic pumps adds the weight and increases the complexity to the system. In addition, under a large payload, the servo motor can still be damaged since it cannot be reversely driven.

Another metric on gripper's performance is the response rate which depends on the diffusion rate of the compressed gas [29]. This also applies to layer jamming which is only effective as the gas is removed from the control volume. By using a high-flow vacuum generator, the response time of a compliant mechanism with layer jamming has been increased to about 0.25 s [27]. Therefore, a pneumatically actuated soft actuator equipped with layer jamming is proposed as the basic configuration of the high adaptability and payload gripper.

In this paper, we present a pneumatically actuated and jammed soft robotic gripper design for achieving both high adaptability and high payload. The shape control is driven by compressed air while the shape locking is activated by a vacuum pressure. The entire finger structure is 3D printed with two materials, which greatly simplifies the fabrication process and reduces the cost.

2 Design Goals and Details

2.1 Motivations and Design Goals. Traditional rigid-body grippers are designed for high performance in terms of large payload and high positioning accuracy, but they also suffer several shortcomings such as low adaptability and high system complexity. On the other hand, recently emerging soft grippers address these shortcomings of rigid-body ones by introducing compliance (using either soft materials or compliant mechanisms) to robotic structures. Soft grippers typically weigh much less due to reduced part count. However, this excellent adaptability is at the cost of performance not only including payload capacity but also positioning accuracy, control bandwidth, etc.

Variable stiffness soft grippers well address these two competing metrics: adaptability and payload performance. While having the advantages of soft grippers, they can be stiffened up for enhanced performance such as carrying a higher payload and reducing energy consumption. An ideal variable stiffness solution should satisfy four main criteria: high load capacity, high adaptability, quick response, and low design overhead (system complexity or extra weight). The current variable stiffness solutions rarely satisfy all these four criteria.

¹Corresponding author.

Contributed by the Mechanisms and Robotics Committee of ASME for publication in the JOURNAL OF MECHANISMS AND ROBOTICS. Manuscript received September 28, 2021; final manuscript received February 6, 2022; published online April 25, 2022. Assoc. Editor: Stephen Canfield.

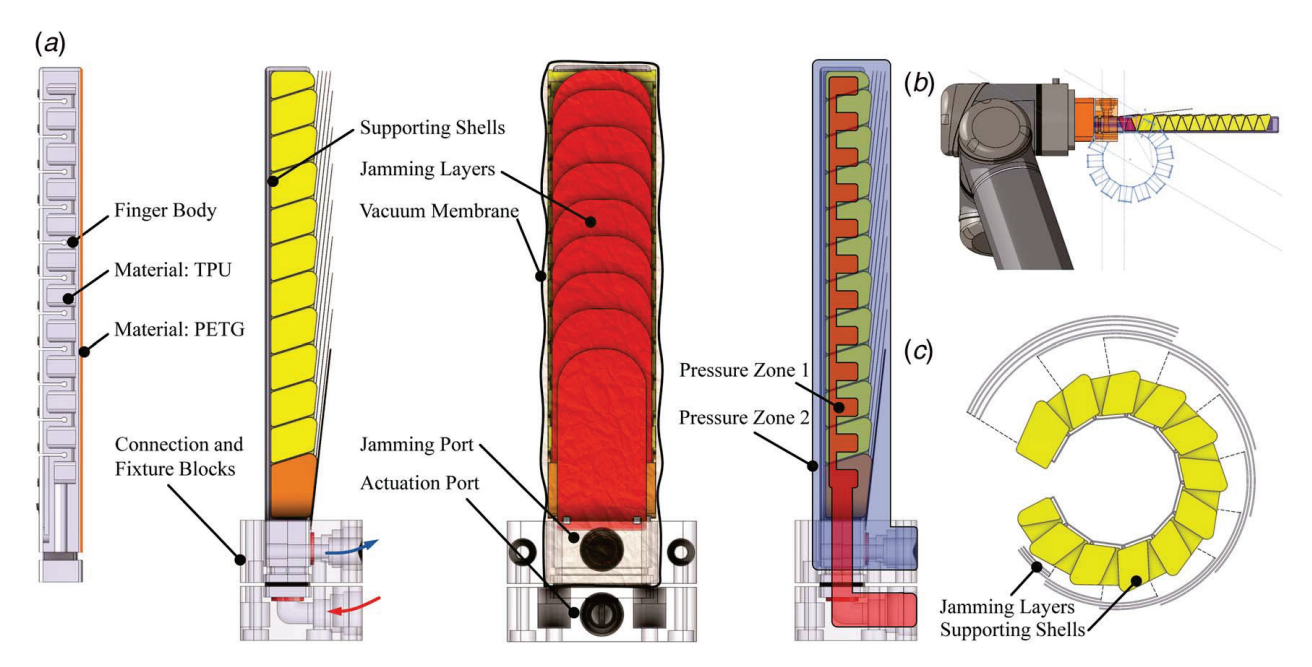


Fig. 1 Design overview; (a) Key components including the finger body, supporting shells, jamming layers, and connection and fixture blocks, (b) the gripper mounted on the UR-5 robotic arm, and (c) the configuration of the support shells and jamming layers

2.2 Design Principles and Details. Here, we present a high performance soft gripper enabled by variable stiffness based on the layer jamming technology [20]. The gripper's actuator or finger is sealed inside a vacuum membrane which is connected to a vacuum source. When the differential pressure across the membrane is created, friction layers are pressed against the finger body. The relative motion of the layers is constrained by the internal friction forces thus locking the finger's shape. This results in a higher structural stiffness, hence a higher payload capacity.

As shown in Fig. 1(a), the design features a 3D printed finger body with one end being clamped in the connection and fixture blocks and the other end being free. The finger body is printed in soft material (60A Shore Hardness, see the next section for fabrication process). By virtue of the inherent cushioning of the soft material, the gripper is expected to conform to objects and obtains robustness by absorbing energy at low cost. Drawing compressed air in and out of pressure zone 1 controls motion. To vacuum down or replenish, the pressure zone 2 controls the payload capacity. The inflation of the soft finger combined with pneumatic-actuated layer jamming is foreseen to resist a higher external load.

A series of supporting shells is fixed to the finger body in order to provide a continuous supporting surface for the jamming layers. Positive pressure, indicated with the arrow pointing into the gripper, is supplied to the actuation port to drive the finger to a desired position. Vacuum pressure is supplied to the jamming port to press the jamming layers, thus enhancing the payload of the finger, which is explained by the blue arrow. Our hypothesis is that (1) large payload capacity enhancement can be achieved by combining layer jamming with flexible finger design, (2) high adaptability is not affected by the extra components such as the supporting shells, jamming layers, and vacuum membrane, (3) quick response of actuation and jamming can be obtained by the design of the internal air channels and the use of the high-glow vacuum generator, respectively, and (4) the system's compactness and ease of control is achievable.

Aside from being the actuator which is driven by compressed air, the soft finger body printed with soft material serves two other purposes: (1) to restore the gripper to its un-deflected shape upon releasing the vacuum pressure and (2) to significantly increase the effectiveness of layer jamming. This is due to the finger body's large thickness which can leverage the resistance moment resulted

from friction forces in jamming layers. The supporting shells, with the functionality illustrated in Fig. 1(c), are critical for the jamming layers to work with the finger body. When the finger body bends, the openings between the adjacent chambers would enlarge. This would create an unsupported portion under the jamming layers. These unsupported layers tend to buckle which would significantly decrease the gripper's payload capacity. With the supporting shells in place, a continuous supporting surface is provided and even the finger bends to its maximum range of motion.

2.3 Functioning Stages. As shown in Fig. 2, the gripper has five functional stages: (1) relaxing (ready to grip), (2) shape actuation (conform to the grasped object), (3) shape locking (stiffened up to secure grip), (4) transportation (hold the object and move with robotic arm), and (5) releasing (release the object to the target area).

The state of valves for each stage is also given in Fig. 2. For instance, the actuation valve is ON and the jamming valve is OFF when the gripper needs to be actuated. Supplying compressed air bends the gripper inwards, letting it wrap around and grip the object. The grasping is done in a form-fitting and gentle manner, a result from using elastic materials including the silicone vacuum membrane and the thermoplastic polyurethane (TPU) finger body. Once the gripper is fully bent under the actuation pressure, the jamming valve is turned on. Venting the air caused the jamming layers to stiffen up and to lock the gripper at the actuated position. Stiffness change from low to high, state (2)-(3), takes 0.25 s due to the high flowrate of the vacuum generator used. The actuation valve can be ON or OFF during the shape locking stage. While the shape locking effectiveness is mostly attributed to the jamming, the actuation pressure can reinforce the locked shape, hence further increases the payload capacity. During the transportation stage, both the actuation and the jamming valves are shut off to prevent air leakage. Once the object reaches the target, both valves exhaust the air, and the object is released.

Now let us discuss the energy consumption of the gripper at different stages. For a conventional rigid-body gripper, energy is consumed throughout the entire process except the "ready to grip" step since the gripper must be active to secure the grip, which is qualitatively graphed in Fig. 2. For our gripper, energy is consumed

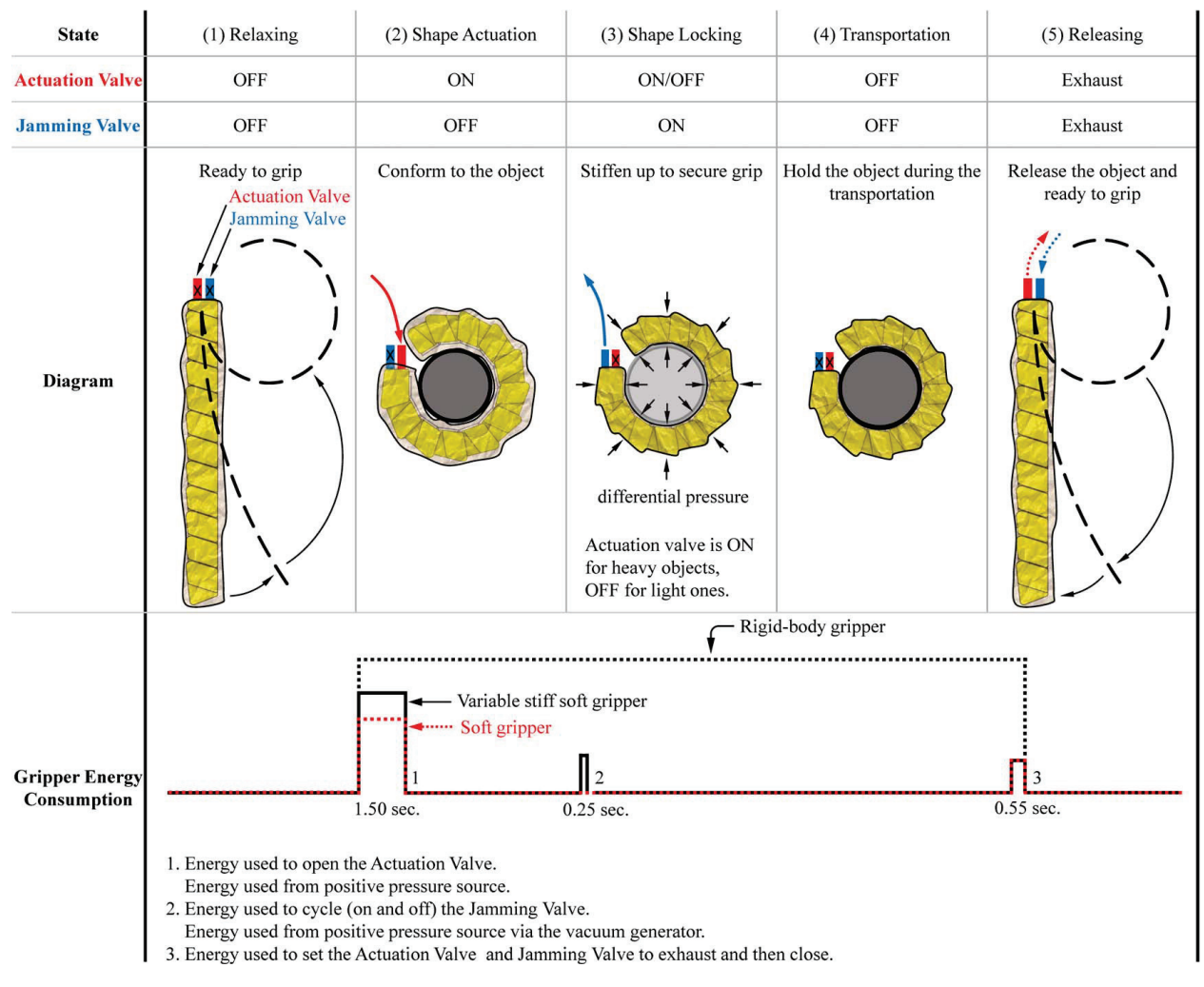


Fig. 2 The schematic view and energy consumption of five functioning stages: (1) relaxing, (2) shape actuation, (3) shape locking, (4) transportation, and (5) releasing

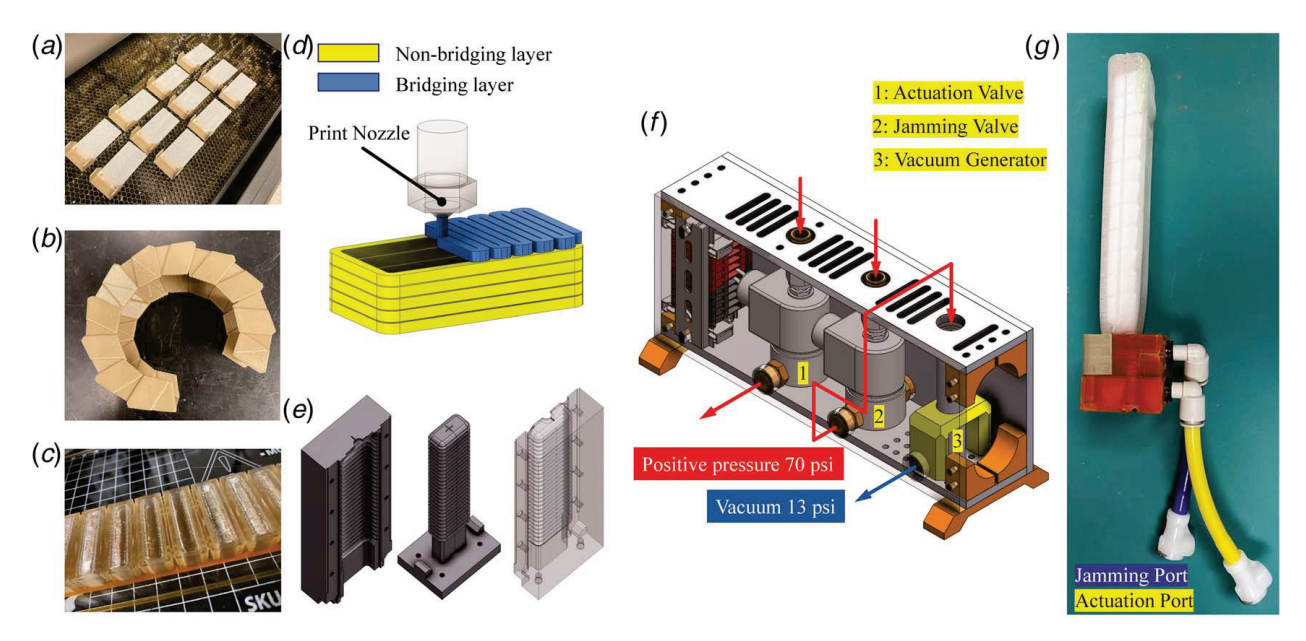


Fig. 3 Fabrication process: (a) assembled shells and jamming layers, (b) testing the supporting shells, (c) printed finger body, (d) bridging process, (e) the mold used to make the silicon vacuum membrane, (f) the valve-box that contains the actuation valve, jamming valve, and vacuum generator, and (g) the assembled prototype

Table 1 3D printing parameters

Parameter	Value or selection TPU Shore Hardness: 60A		
Material			
Nozzle temperature	225 °C		
Bed temperature	80 °C		
Support	None		
Layer height	0.1 mm		
Perimeters	3		
Infill	100%		
Perimeter speed	20 mm/s		
Bridges speed	5 mm/s		
Non-print move speed	200 mm/s		
Cooling fan speed	0%		
Bridges fan speed	100%		
Extrusion multiplier	1.25		

only for the two steps: "shape conforming" and "securing grip." Once a robust grip is secured, the vacuum source can be shut off (with valves remaining closed to maintain the vacuum) for picking up and transportation. Theoretically, it consumes zero energy during the transportation stage which is the most energy consuming one of the entire functioning cycle. Moreover, during the "releasing object" step, only a short burst of electric energy is consumed to exhaust the actuation valve and jamming valve to the atmosphere. The restoration to the un-deflected position is realized by the compliant structure of the gripper.

Comparing with a pure soft gripper, a variable stiffness gripper equipped with layer jamming needs to consume slightly more energy such as using higher actuation pressure to stretch the vacuum membrane. The layer jamming gripper has no energy consumption advantage over a soft gripper when picking up small weights. The real advantage of layer jamming gripper is to grip heavy objects which a soft gripper is unable to handle.

3 Fabrication Process and Prototype

The design aims to serve as a universal gripper on industrial robot that handles medium-duty tasks (5–10 kg payload) such as UR-5.

The dimensions are determined in the way that the prototype can be readily connected on UR-5's mounting flange. Figure 1(b) shows the proposed robotic gripper mounted on the UR-5.

Figure 3 shows the overall fabrication workflow: (a) 3D printed supporting shells (material: polyethylene terephthalate glycol (PETG)) and laser cut jamming layers (material: polyethylene) are joined with adhesive. (b) The supporting shells are temporally assembled to test the dimension tolerance. (c) The finger body is 3D printed with two materials. The thin layer on the bottom of the finger body is printed in polyethylene terephthalate glycol (PETG) that aims to increase the rebound elasticity and stability. The soft transparent material, thermoplastic polyurethane (TPU), is used to print the air-tight chambers and channels. CoexFlex™ 60A TPU is selected due to its high tensile strength (35 MPa), excellent tear strength (40 N/mm), and good wear performance. (d) The bridging of soft TPU is difficult. To have the top of the chambers properly sealed, the bridging process must be configured with extra slow print speed and high cooling flow. Table 1 summarizes the key print parameters. The complex internal structures including the chambers and channels would be very difficult to make with molding method. 3D-printing allows fast design and test iterations by changing the design parameters. (e) Vacuum membrane is made with a silicone rubber molding process. The vacuum membrane needs to be air-tight to maintain the vacuum pressure and needs to be extremely elastic to not constrain the bending motion of the finger. Dragon Skin 20 silicon is selected as the membrane material due to its high tear strength, low modulus, and high elongation. (f) For quick response, both actuation and jamming have been optimized. The actuation valve is connected to a compressed air source capable of supplying air at 70 psi with the flowrate of 10 cubic feet per minute (cfm). The vacuum created by the vacuum generator can bring down the jamming pressure to -12.5 psi with the maximum flowrate of 1.2 cfm. Internal channels have also been designed to facilitate fast air moving.

The final prototype is assembled without any moving parts and is weighed at only 522 g including the interface base and tubings, and only 231 g for the finger body.

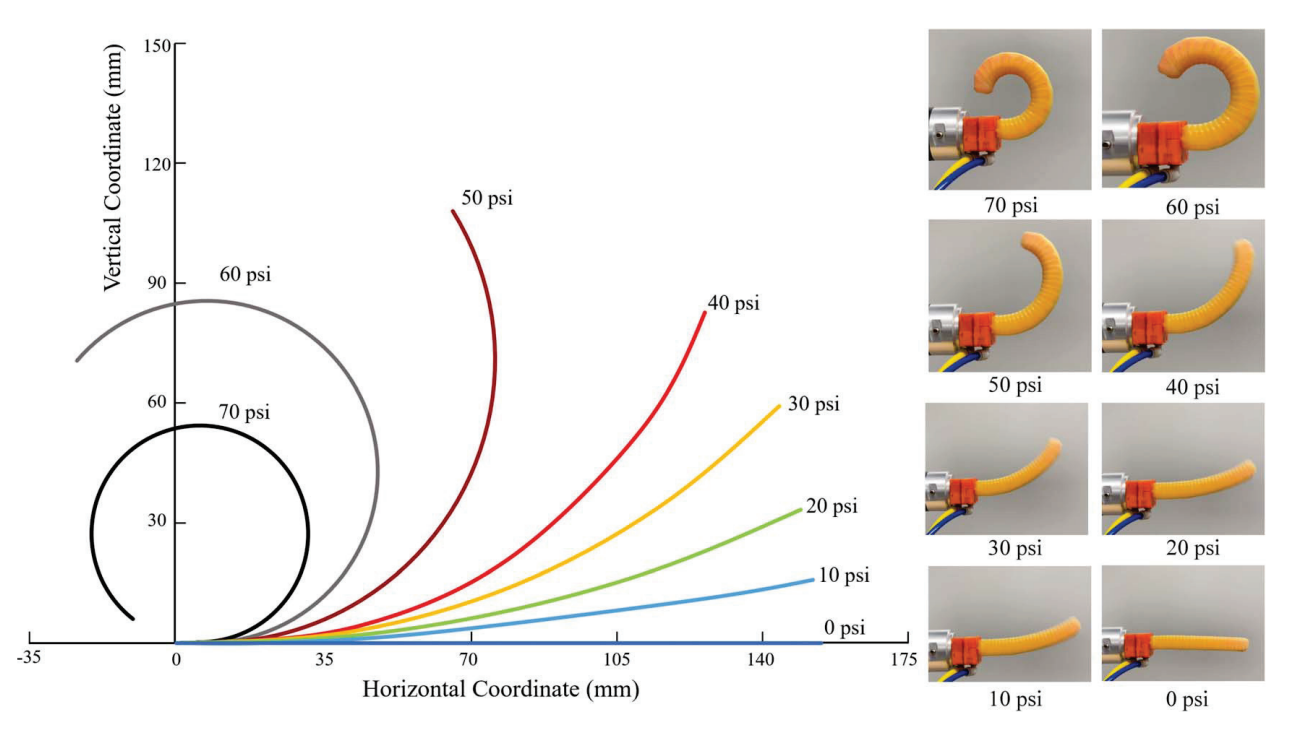


Fig. 4 Gripper shapes corresponding to actuation pressures

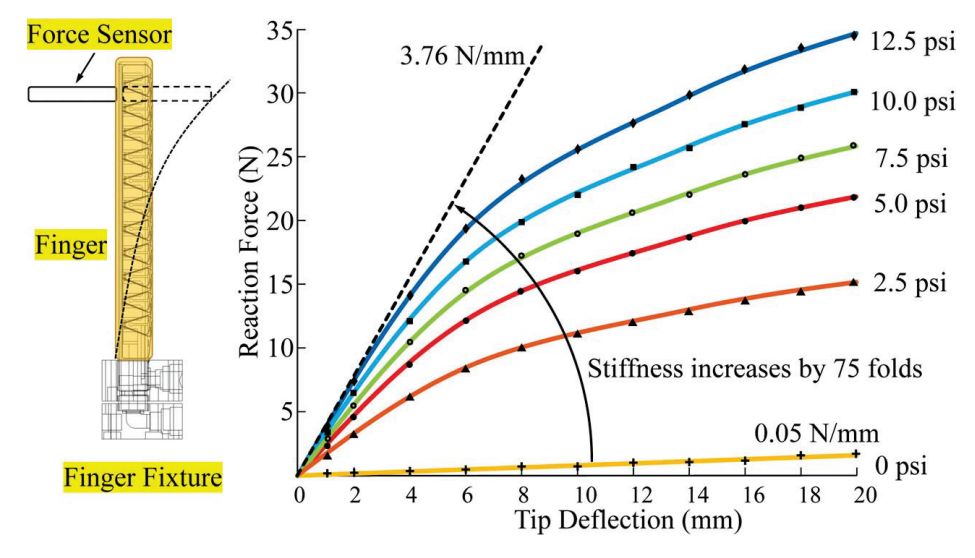


Fig. 5 Stiffness variation test: the tip loading force versus the tip deflection

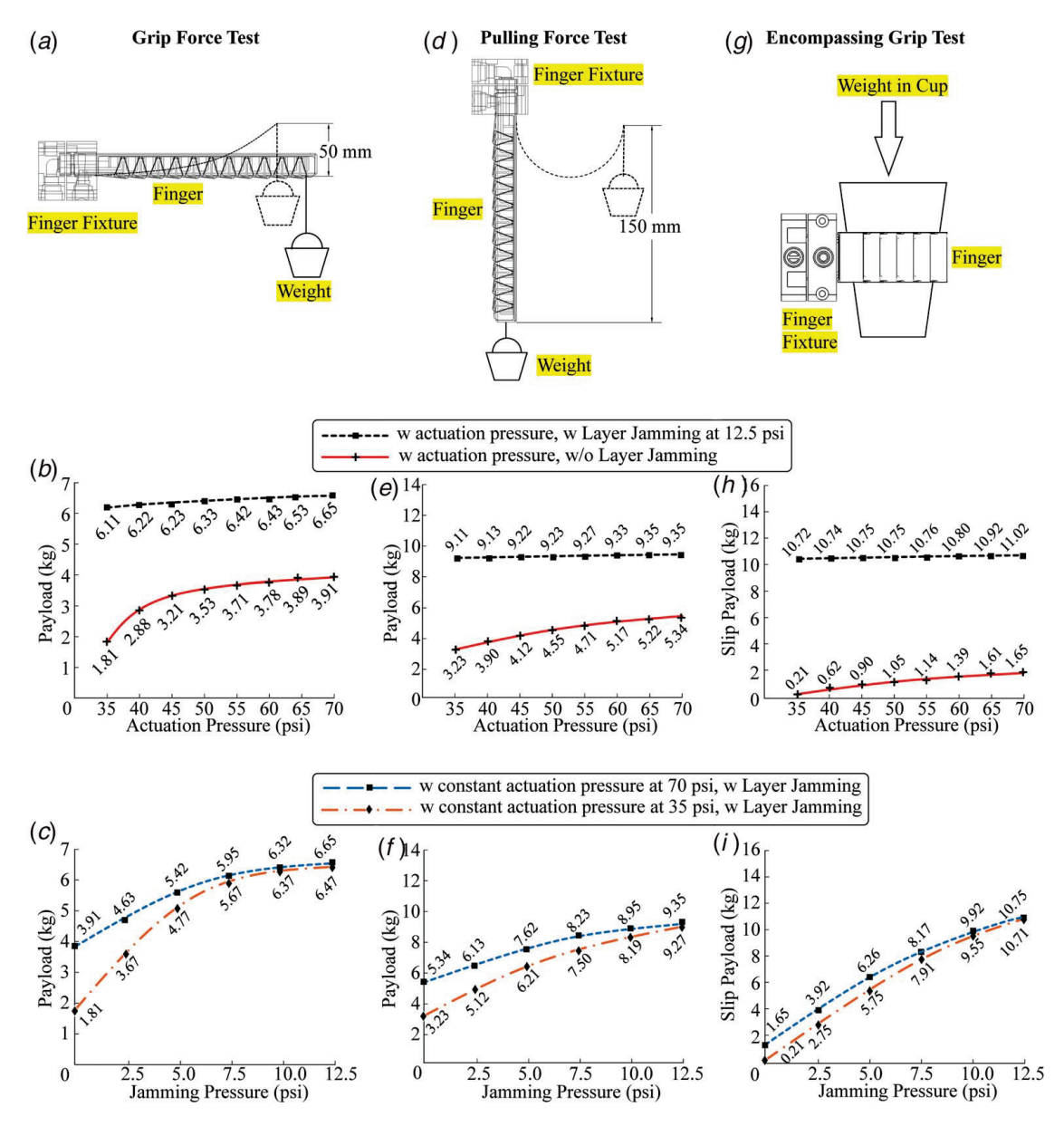


Fig. 6 Payload capacity tests with and without layer jamming. (a)–(c) Grip force test. (d)–(f) Pulling force test. (g)–(i) Encompassing grip test.

Table 2 Payload capacity improvement with LJ (layer jamming)

	Payload (kg)						
	Actuation pressure: 35 psi			Actuation pressure: 70 psi			
Payload test	Without LJ	With LJ	× Times increase	Without LJ	With LJ	×Times increase	
Grip force test Pulling force test Encompassing test	1.81 3.23 0.21	6.47 9.27 10.71	3.57 2.87 51.00	3.91 5.34 1.65	6.65 9.35 11.02	1.70 1.75 6.68	

4 Performance Evaluation

4.1 Actuation Tests. In this section, a series of metrics including blocking force, stiffness, and payload capacities in various working configurations are measured.

The gripper is actuated from 10 psi to 70 psi with an increment of 10 psi. A fixed camera is used to capture the videos of the actuated gripper. An object position tracking software, named Tracker, is used to extract the shape information. Figure 4 summarizes the gripper shapes corresponding to input pressures. The vacuum pressure is not supplied to engage the layers during this test. This is due to the decoupled actuation and stiffness change of the gripper meaning the stiffness change only occurs until the gripper moves

to the target position. Therefore, the stiffness variation has no impact on the range of motion of the gripper. The gripper can bend to almost a full circle at 70 psi. The gripper is rated to handle 85 psi by destructive tests on several prototypes. The upper limit of the actuation pressure is then limited to 70 psi for safety concern.

4.2 Stiffness Variation Tests. To measure the effect of the layer jamming, the following test is designed. On the left portion of Fig. 5, the gripper is fixed through the finger fixture. The force sensor combined with a deflection sensor moves laterally pushing the tip of the gripper and measuring the reaction force or the tip loading force versus the tip deflection. This test measures the



Fig. 7 Selected demonstrations showing the high adaptation feature of the gripper (LJ stands for layer jamming, ON and OFF indicate the actuation status of layer jamming)

resistance of the gripper to the external lateral load. A large external load with the gripper bending to the same deflection (20 mm) indicates a higher load resistance.

4.3 Payload Tests. The following three payload tests aim to benchmark the gripper in three typical load carrying task settings.

Multiple data collections are made from 0 psi (0 Pa) to 12.5 psi (86.2 kPa) with an increment of 2.5 psi (17.2 kPa). Under these vacuum pressures, the reaction force-tip deflection curves are drawn. With vacuum pressure at 0 psi (vacuum pressure is not applied), the external load increases linearly with tip deflection resulting in a constant stiffness of 0.0503 N/mm. This is due to the layer material's low friction characteristic that minimizes the jamming effect under zero pressure. For non-zero vacuum pressures, the curves exhibit three loading phases. The curve with the vacuum pressure at 12.5 psi, for instance, initially rises linearly with a slope of 3.76 N/mm (non-slipping phase), then advances non-linearly (transitional phase) represented by the curvy transitional section between 4 mm and 10 mm. And finally, the curve progresses linearly again but with a lower slope than that of non-slipping phase. Under small deflection, the non-slipping phase slopes increase by 75 folds from un-jammed to fully jammed state. The large stiffness variation is expected to enhance the payload capacity of the gripper, when the layers are fully jammed, but without affecting the adaptability.

The first test is called "grip force test" which measures the pinching force at the fingertip as shown in Figs. 6(a)–6(c). In Fig. 6(a), the gripper is oriented horizontally with a container attached to the gripper tip. The initial actuation pressure is supplied so the gripper bends up. Then weight is gradually added to the container to lower the gripper tip. When the gripper tip reaches the 50 mm height, the weight is recorded. Figure 6(b) shows that without layer jamming, the payload is positive proportional with the actuation pressure. The payload reaches its max value of 3.91 kg at 70 psi actuation pressure. With layer jamming enabled, the payload capacity jumps to around 6 kg. With the flat curve, it indicates that the payload capacity in this setting is dominated by the jamming effect rather than the actuation pressure. This finding is further investigated by fixing the actuation pressure at 35 psi and 70 psi and test the payload capacity with respect to the jamming pressure. Figure 6(c) shows that without jamming pressure, at jamming pressure at 0 psi, the payload is closely dependent on the actuation pressure. But with jamming fully enabled, even with the minimum and maximum pressure enabled respectively, the payload capacity is mainly dominated by the jamming effect.

The second one is called "pulling force test," which measures how much weight the gripper can pull up. The gripper is oriented vertically down as shown in Fig. 6(d). Similarly, a container is attached to the gripper tip. The initial actuation pressure is supplied so the gripper curls up. Then weight is gradually added to the container to lower the gripper tip. When the gripper tip reaches the 150 mm height, the weight is recorded. Similar trend on payload capacity is observed. The payload increases with actuation pressure without the jamming layers enabled. The payload curve flattens out with jamming enabled with payload capacity almost doubled.

The last one is called "encompassing grip test" which is designed to test the gripping capacity of enclosing a round shape. The gripper initially bends and surrounds a slightly tapered cup which holds extra weight inside. We then gradually add weight to the cup until the cup fully slips off the grip. This final weight is defined as the slip payload. Figure 6(h) shows that even at the maximum actuation pressure, the gripper can only grip 1.65 kg weight in the cup. But with layer jamming enabled, the slip capacity jumps up to around 11 kg. This significant increase in slip payload is due to the large stiffness change of the gripper in the gripping configuration. Also, from Fig. 6(i), it is seen that at the higher end of the slip payload, the dominant factor is the jamming pressure. At the lower end of the slip payload, the actuation pressure is the dominant factor instead.

Table 2 summarizes the overall performance improvement of all three payload tests. By utilizing the layer jamming (at vacuum pressure 12.5 psi), the payload capacity of the gripper has been increased from 2.87 to 51 folds at actuation pressure of 35 psi and from 1.7 to 6.68 folds at actuation pressure of 70 psi. As one can see, its payload capacity in the grip force test is much higher than that of soft grippers (mGrip P2 from soft robotics grips 0.8 kg and weighs 334 g), even higher than some small-scale rigid-body grippers (Hand-E from ROBOTIQ grips 5 kg and weighs 1 kg).

4.4 Adaptability Tests. To demonstrate the high adaptation, we ran tests of many grasping cases. Some of them are shown in Fig. 7. In all gripping demonstrations, the gripper does not need to be precisely positioned and oriented. A simple "on" signal is sent to the solenoid valve to release the pre-regulated pressured air. This simplifies the gripping control compared to most rigid grippers.

In Figs. 7(b) and 7(c), the gripper presents two different gripping postures under the same input pressure and same simple control algorithm. The gripper also exhibits high payload capacity as shown in Figs. 7(a), 7(d), and 7(e). In these cases, once the gripper closes its form and adapts to the shape of the objects, the

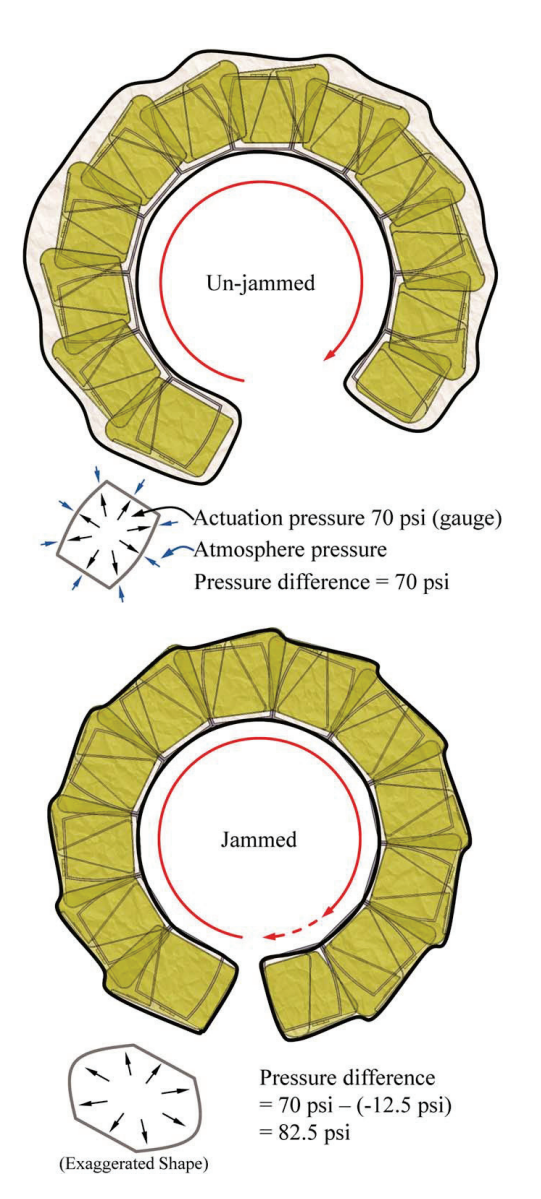


Fig. 8 The extra grip when the layers are jammed

vacuum port is opened to remove the air from the jamming membrane. This results in two effects: first, the differential pressure across the jamming membrane presses the jamming layers, thus stiffens the gripper; second, the differential pressure across the actuation chamber is further increased by this vacuum. The gripper bends even more due to the increased differential pressure providing an extra grip while the gripper is being stiffened. An illustrative explanation of the mechanism is presented in Fig. 8. The extra grip is preferable in the friction gripping cases in which the friction force balances the weight, such as the cases in Figs. 7(a), 7(e), 7(g), and 7(i). See the supplemental video available in the Supplemental Materials on the ASME Digital Collection for more demonstrations and grasping cases.

From these tests, we conclude that our gripper is as good as most soft grippers in terms of gripping objects with various shapes. However, our gripper is much stronger than all current soft grippers as shown in the payload tests.

5 Conclusions

This study demonstrates that layer jamming as the technique of actively tuning the stiffness, combined with 3D printed soft finger, is an effective approach for improving payload capacity of soft grippers. The prototype is flexible enough to grip a broad range of geometries, exhibits high payload capacity, holds objects in place without consuming energy, and requires minimal control effort. It combines the advantages of soft and rigid-body grippers and achieves both high adaptability and high payload capacity. Weighted at around 522 g, this design features an exceptional high payload capacity (6-10 kg), and a very high response speed without affecting the compactness of the gripper. The novelty lies in (1) the use of 3D printed extremely soft material with the shore hardness of 60A which allows the large actuation range under a reasonable actuation pressure and (2) the design of the supporting shells that provide a continuous supporting surface for the jamming layers without constraining the range of motion of the gripper. We conclude that the proposed gripper is as adaptive as most soft grippers even with the one-finger configuration. Moreover, the proposed gripper has much higher payload than all current soft grippers.

Acknowledgment

This material is based upon work supported by the National Science Foundation under Grant No. 2019648. Any opinions, findings, and conclusions or recommendations expressed in this material are those of the author(s) and do not necessarily reflect the views of the funding agencies.

Conflict of Interest

There are no conflicts of interest.

Data Availability Statement

The authors attest that all data for this study are included in the paper.

References

- Rus, D., and Tolley, M. T., 2015, "Design, Fabrication and Control of Soft Robots," Nature, 521(7553), pp. 467–475.
- [2] Laschi, C., and Cianchetti, M., 2014, "Soft Robotics: New Perspectives for Robot Bodyware and Control," Front. Bioeng. Biotechnol., 2(3), pp. 1–2.
- [3] Pfeifer, R., Lungarella, M., and Iida, F., 2012, "The Challenges Ahead for Bio-Inspired 'Soft' Robotics," Commun. ACM, 55(11), pp. 76–87.
- [4] Trivedi, D., Rahn, C. D., Kier, W. M., and Walker, I. D., 2008, "Soft Robotics: Biological Inspiration, State of the Art, and Future Research," Appl. Bionics Biomech., 5(3), pp. 99–117.

- [5] Wood, R., and Walsh, C., 2013, "Smaller, Softer, Safer, Smarter Robots," Sci. Transl. Med., 5(210), p. 210ed19.
- [6] Zhang, J., Sheng, J., O'Neill, C. T., Walsh, C. J., Wood, R. J., Ryu, J.-H., Desai, J. P., and Yip, M. C., 2019, "Robotic Artificial Muscles: Current Progress and Future Perspectives," IEEE Trans. Rob., 35(3), pp. 761–781.
- [7] Li, Y., Chen, Y., and Li, Y., 2019, "Pre-Charged Pneumatic Soft Gripper With Closed-Loop Control," IEEE Rob. Autom. Lett., 4(2), pp. 1402–1408.
- [8] Blanc, L., Delchambre, A., and Lambert, P., 2017, "Flexible Medical Devices: Review of Controllable Stiffness Solutions," Actuators, 6(3), p. 23.
- [9] She, Y., Su, H.-J., Lai, C., and Meng, D., 2016, "Design and Prototype of a Tunable Stiffness Arm for Safe Human–Robot Interaction," Volume 5B: 40th Mechanisms and Robotics Conference, Charlotte, NC, Aug. 21–24, p. V05BT07A063.
- [10] Schubert, B. E., and Floreano, D., 2013, "Variable Stiffness Material Based on Rigid Low-Melting-Point-Alloy Microstructures Embedded in Soft Poly(Dimethylsiloxane) (PDMS)," RSC Adv., 3(46), p. 24671.
- [11] Sun, S. S., Chen, Y., Yang, J., Tian, T. F., Deng, H. X., Li, W. H., Du, H., and Alici, G., 2014, "The Development of an Adaptive Tuned Magnetorheological Elastomer Absorber Working in Squeeze Mode," Smart Mater. Struct., 23(7), p. 075009.
- [12] Hauser, S., Robertson, M., Ijspeert, A., and Paik, J., 2017, "JammJoint: A Variable Stiffness Device Based on Granular Jamming for Wearable Joint Support," IEEE Rob. Autom. Lett., 2(2), pp. 849–855.
- [13] Brown, E., Rodenberg, N., Amend, J., Mozeika, A., Steltz, E., Zakin, M. R., Lipson, H., and Jaeger, H. M., 2010, "Universal Robotic Gripper Based on the Jamming of Granular Material," Proc. Natl. Acad. Sci. U.S.A., 107(44), pp. 18809–18814.
- [14] Cheng, N. G., Lobovsky, M. B., Keating, S. J., Setapen, A. M., Gero, K. I., Hosoi, A. E., and Iagnemma, K. D., 2012, "Design and Analysis of a Robust, Low-Cost, Highly Articulated Manipulator Enabled by Jamming of Granular Media," 2012 IEEE International Conference on Robotics and Automation, Saint Paul, MN, May 14–18, IEEE, pp. 4328–4333.
- [15] Jiang, A., Xynogalas, G., Dasgupta, P., Althoefer, K., and Nanayakkara, T., 2012, "Design of a Variable Stiffness Flexible Manipulator With Composite Granular Jamming and Membrane Coupling," 2012 IEEE/RSJ International Conference on Intelligent Robots and Systems, Vilamoura-Algarve, Portugal, Oct. 7–12, IEEE, pp. 2922–2927.
- [16] Ranzani, T., Cianchetti, M., Gerboni, G., Falco, I. D., Petroni, G., and Menciassi, A., "A Modular Soft Manipulator With Variable Stiffness," 3rd Joint Workshop on New Technologies for Computer/Robot Assisted Surgery, Verona, Italy, Sept. 11–13, p. 4.
- [17] Ranzani, T., Cianchetti, M., Gerboni, G., Falco, I. D., and Menciassi, A., 2016, "A Soft Modular Manipulator for Minimally Invasive Surgery: Design and Characterization of a Single Module," IEEE Trans. Rob., 32(1), pp. 187–200.
- [18] Brancadoro, M., Manti, M., Tognarelli, S., and Cianchetti, M., 2018, "Preliminary Experimental Study on Variable Stiffness Structures Based on Fiber Jamming for Soft Robots," 2018 IEEE International Conference on Soft Robotics (RoboSoft), Livorno, Italy, Apr. 24–28, IEEE, pp. 258–263.
- [19] Ou, J., Yao, L., Tauber, D., Steimle, J., Niiyama, R., and Ishii, H., 2013, "jamSheets: Thin Interfaces With Tunable Stiffness Enabled by Layer Jamming," Proceedings of the 8th International Conference on Tangible, Embedded and Embodied Interaction—TEI '14, Munich, Germany, Feb. 16–19, ACM Press, pp. 65–72.
- [20] Kim, Y.-J., Cheng, S., Kim, S., and Iagnemma, K., 2012, "Design of a Tubular Snake-Like Manipulator With Stiffening Capability by Layer Jamming," 2012 IEEE/RSJ International Conference on Intelligent Robots and Systems, Vilamoura-Algarve, Portugal, Oct. 7–12, IEEE, pp. 4251–4256.
- [21] Kim, Y., Cheng, S., Kim, S., and Iagnemma, K., 2013, "A Novel Layer Jamming Mechanism With Tunable Stiffness Capability for Minimally Invasive Surgery," IEEE Trans. Rob., 29(4), pp. 1031–1042.
- [22] Santiago, J. L. C., Godage, I. S., and Walker, I. D., 2016, "Soft Robots and Kangaroo Tails: Modulating Compliance in Continuum Structures Via Mechanical Layer Jamming," Soft Rob., 3(2), pp. 54–63.
- [23] Deshpande, A. R., Tse, Z. T. H., and Ren, H., 2017, "Origami-Inspired Bi-Directional Soft Pneumatic Actuator With Integrated Variable Stiffness Mechanism," 2017 18th International Conference on Advanced Robotics (ICAR), Hong Kong, China, July 10–12, IEEE, pp. 417–421.
- [24] Hadi Sadati, S. M., Noh, Y., Elnaz Naghibi, S., Kaspar, A., and Nanayakkara, T., 2015, "Stiffness Control of Soft Robotic Manipulator for Minimally Invasive Surgery (MIS) Using Scale Jamming," *Intelligent Robotics and Applications*, Liu, H., Kubota, N., Zhu, X., Dillmann, R., and Zhou, D., eds., Vol. 9246, Springer International Publishing, Cham, pp. 141–151.
- [25] Tognarelli, S., Brancadoro, M., Dolosor, V., and Menciassi, A., 2018, "Soft Tool for Gallbladder Retraction in Minimally Invasive Surgery Based on Layer Jamming," 2018 7th IEEE International Conference on Biomedical Robotics and Biomechatronics (Biorob), Enschede, Netherlands, Aug. 26–29, IEEE, pp. 67–72.
- [26] Amanov, E., Nguyen, T.-D., Markmann, S., Imkamp, F., and Burgner-Kahrs, J., 2018, "Toward a Flexible Variable Stiffness Endoport for Single-Site Partial Nephrectomy," Ann. Biomed. Eng., 46(10), pp. 1498–1510.
- [27] Zeng, X., Hurd, C., Su, H.-J., Song, S., and Wang, J., 2020, "A Parallel-Guided Compliant Mechanism With Variable Stiffness Based on Layer Jamming," Mech. Mach. Theory, 148, p. 103791.
- [28] Gao, Y., Huang, X., Mann, I. S., and Su, H.-J., 2020, "A Novel Variable Stiffness Compliant Robotic Gripper Based on Layer Jamming," ASME J. Mech. Rob., 12(5), p. 051013.